

Fermionic superfluid from a bilayer band insulator in an optical lattice

Yogeshwar Prasad,¹ Amal Medhi,^{1,2} and Vijay B. Shenoy^{1,*}

¹Center for Condensed Matter Theory, Indian Institute of Science, Bangalore 560012, India

²School of Physics, IISER Thiruvananthapuram, CET Campus, Thiruvananthapuram 695016, India

(Received 1 March 2014; published 7 April 2014)

We propose a model to realize a fermionic superfluid state in an optical lattice circumventing the cooling problem. Our proposal exploits the idea of tuning the interaction in a characteristically low-entropy state, a band insulator in an optical bilayer system, to obtain a superfluid. By performing a detailed analysis of the model including fluctuations and augmented by a variational quantum Monte Carlo calculation of the ground state, we show that the superfluid state obtained has a high transition temperature of the order of the hopping energy. Our system is designed to suppress other competing orders such as a charge density wave. We suggest a laboratory realization of this model via an orthogonally shaken optical lattice bilayer.

DOI: [10.1103/PhysRevA.89.043605](https://doi.org/10.1103/PhysRevA.89.043605)

PACS number(s): 03.75.Kk, 71.10.Fd, 37.10.Jk, 74.78.Fk

I. INTRODUCTION

Quantum emulation of interesting condensed matter Hamiltonians using ultracold atom systems holds much promise [1–5]. The pace of experimental progress has been impeded by key problems which include simulation of electromagnetic (gauge) fields, removal of entropy, etc. While the former has seen spectacular recent progress [6–10], the longstanding “cooling problem” of trapped lattice fermions has been more difficult [11].

The cooling problem has been addressed in various ways. One approach has been to find schemes to “squeeze out” the entropy [12–15]. Others include exploiting metastable states [16], using properties of the states (such as the Néel state) to develop cooling protocols [17] (see Ref. [11] for a review). A recent notable proposal is to use an additional beam that helps to enlarge the region where a desired state is stabilized [18]. Despite this, to the best of our knowledge, an interesting many-body state such as an antiferromagnet is yet to be realized in an optical lattice, while some signatures of fermionic superfluidity have been reported [19].

We propose here an alternate strategy to address the entropy problem which hinges on using a *low-entropy* noninteracting state as a starting point. Such a low-entropy state, which will be formed in the central region of a trap in a cold-atom system, has the benefit that it allows for the spatial separation of the excess entropy that will be accommodated in the periphery of the trap. Upon tuning an interaction, the low-entropy state in the central region is driven to an interesting many-body state which has the desiderata of (i) a high characteristic temperature scale and (ii) stability over other “uninteresting” competing states. Here we suggest the use of a *band insulator*, a characteristically low-entropy state in which we tune an attractive interaction to produce a fermionic superfluid utilizing the above strategy. Band-insulator–superfluid transitions have been investigated earlier in other contexts [20,21]. Motivated by the experimental work cited above [19], band-insulator–superfluid transitions, in fermionic cold-atom systems, engendered by increasing the lattice depth with concomitant multiband effects have been

discussed [22–26]. In contrast to these works, our proposal aims to obtain a superfluid in a deep lattice.

We propose and study a *bilayer band insulator* that undergoes a transition to a superfluid upon tuning an attractive interaction, attaining the above desiderata. The model is designed so that competing phases, such as the charge density wave (CDW), are avoided. This is demonstrated by a detailed analysis including Gaussian fluctuations and variational Monte Carlo simulations. We show that a “high-temperature” superconducting phase is possible in this system by estimating the Berezinski-Kosterlitz-Thouless transition temperature T_{BKT} . In a regime of parameters, the system shows interesting physics such as the “pseudogap phenomenon,” even at high temperatures. We suggest a possible route to realize this in an optical lattice.

II. BILAYER BAND INSULATOR

Our proposal for the realization of a two-dimensional (2D) spin- $\frac{1}{2}$ fermionic superfluid state hinges on a bilayer band insulator. The configuration consists of two layers, A and B , both of which have the same lattice structure (such as a square or triangular lattice) and a 2D Brillouin zone (see Fig. 1). The crucial ingredient is that the in-plane energy dispersion in the two layers are of *opposite* signs, i.e., $\varepsilon_A(\mathbf{k}) = -\varepsilon_B(\mathbf{k}) = \varepsilon(\mathbf{k})$ for all \mathbf{k} in the Brillouin zone. Interlayer hopping is described by a hybridization function, $h(\mathbf{k})$, which is such that $h(\mathbf{k})$ and $\varepsilon(\mathbf{k})$ never vanish simultaneously. The kinetic energy of the system is thus described by $\mathcal{H}_K = \sum_{\mathbf{k}\sigma} \varepsilon(\mathbf{k})(a_{\mathbf{k}\sigma}^\dagger a_{\mathbf{k}\sigma} - b_{\mathbf{k}\sigma}^\dagger b_{\mathbf{k}\sigma}) + (h(\mathbf{k})a_{\mathbf{k}\sigma}^\dagger b_{\mathbf{k}\sigma} + \text{H.c.})$, where a 's and b 's are spin- $\frac{1}{2}$ fermion operators corresponding to the A and B layers, respectively ($\sigma = \uparrow, \downarrow$ is the spin). This leads to two (spin degenerate) bands:

$$\mathcal{H}_K = \sum_{\mathbf{k}\sigma} e(\mathbf{k})(c_{\mathbf{k}\sigma}^\dagger c_{\mathbf{k}\sigma} - d_{\mathbf{k}\sigma}^\dagger d_{\mathbf{k}\sigma}), \quad (1)$$

where $c_{\mathbf{k}\sigma} = f_{\mathbf{k}}^* a_{\mathbf{k}\sigma} + g_{\mathbf{k}}^* b_{\mathbf{k}\sigma}$ and $d_{\mathbf{k}\sigma} = -g_{\mathbf{k}} a_{\mathbf{k}\sigma} + f_{\mathbf{k}} b_{\mathbf{k}\sigma}$ [$f_{\mathbf{k}}, g_{\mathbf{k}} = \frac{1}{\sqrt{2}}(1 \pm \frac{\varepsilon(\mathbf{k})}{e(\mathbf{k})})^{1/2} e^{\pm i \arg h(\mathbf{k})/2}$] are, respectively, “conduction” and “valence” band fermion operators, with $e(\mathbf{k}) = \sqrt{\varepsilon(\mathbf{k})^2 + |h(\mathbf{k})|^2}$. With a fermion density of one particle per site on both the A and B layers, the ground state is the filled valance band, i.e., a band insulator.

*shenoy@physics.iisc.ernet.in

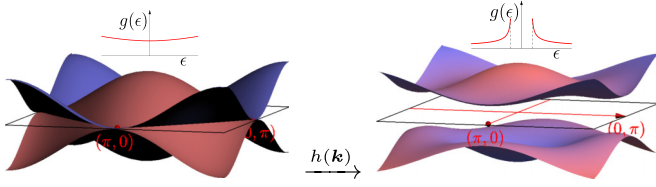


FIG. 1. (Color online) Dispersion of the bilayer band insulator. Bilayer dispersion before (left) and after (right) interlayer hybridization. Insets show the schematic densities of states.

III. SUPERFLUID STATE IN THE BILAYER BAND INSULATOR

We now introduce a local *attractive* interaction with strength U (which may be tuned by a Feshbach resonance [27]) as

$$\mathcal{H}_U = -U \sum_i (a_{i\uparrow}^\dagger a_{i\downarrow}^\dagger a_{i\downarrow} a_{i\uparrow} + b_{i\uparrow}^\dagger b_{i\downarrow}^\dagger b_{i\downarrow} b_{i\uparrow}). \quad (2)$$

A superfluid can be generated by starting from the band insulator ($U \approx 0$) and adiabatically increasing the magnitude of the attractive interaction. To be specific, we choose a particular model to illustrate the idea (see below for a possible laboratory realization of this model). The bilayer system has both A and B layers which are square lattices (of unit lattice spacing) with nearest (t) and next-nearest (t') hopping ($t' = t/10$ throughout) such that $\varepsilon_A(\mathbf{k}) = -\varepsilon_B(\mathbf{k}) = \varepsilon(\mathbf{k}) = -2t(\cos k_x + \cos k_y) - 4t' \cos k_x \cos k_y$. The hybridization function $h(\mathbf{k}) = -t_h$ captures the hopping from adjacent A and B sites. The resulting band structure is of the form in Eq. (1) and has a band gap of $\epsilon_g = 2t_h$. The band insulator obtained with one particle per site per layer has a Cooper instability [28] at a nonzero critical value U_c of U unlike in a metal where U_c is zero. We find that $\frac{1}{U_c} \approx \frac{1}{N} \sum_k \frac{1}{e(k)} \sim \frac{1}{t} |\ln \frac{t}{\epsilon_g}|$ (see Fig. 2), where N is the number of sites per layer. The instability is due to the fact that, at sufficiently large U , it becomes feasible for a pair of fermions of opposite spin to be promoted to a conduction band where they can “sample” the attractive interaction [see Fig. 2(a)], eventually forming a bound state. We find that for $U \gtrsim U_c$, the binding energy of the pair goes as $(U - U_c)$, which may be contrasted with an exponentially small value usually found [28] in a system with a Fermi surface. The physics of such strong binding is due to the modification of the density of states at the band edges engendered by the hybridization. The resulting joint density of states of particle-hole excitations is strongly enhanced (see Fig. 1), $g(\epsilon) \sim 1/\sqrt{\epsilon - \epsilon_g}$, and it is this large enhancement

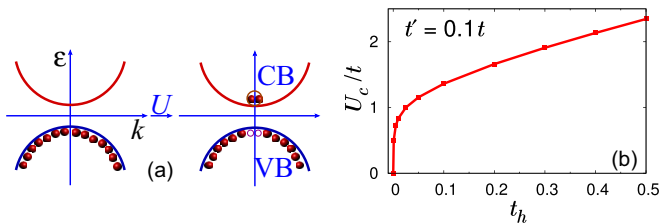


FIG. 2. (Color online) (a) Schematic of Cooper instability. (b) The critical value U_c that induces Cooper instability.

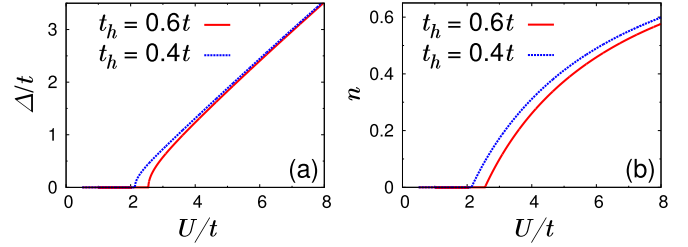


FIG. 3. (Color online) Dependence of zero temperature (a) superfluid order parameter Δ and (b) “carrier density” n on U .

that provides for the strong binding as in other contexts [29]. Consequently we expect the system to also possess high transition temperatures making it attractive for experimental realization of an optical lattice superfluid.

We now study the properties of the lattice superfluid state using functional integral techniques [30,31], by introducing the action

$$\begin{aligned} S[\psi] = & \sum_{k,\alpha} \psi_{\alpha\sigma}^*(k) [-G_0^{-1}(k)] \psi_{\alpha\sigma}(k) \\ & + \sum_k [h(\mathbf{k}) \psi_{1\sigma}^*(k) \psi_{1\sigma}(k) + \text{g.c.}] \\ & - \frac{U}{\beta N} \sum_{q,\alpha} P_\alpha^*(q) P_\alpha(q), \end{aligned} \quad (3)$$

where $-G_0^{-1}(k) = (-ik_n + \alpha\varepsilon(\mathbf{k}) - \mu)$, μ is the chemical potential, $k = (ik_n, \mathbf{k})$ and (iq_ℓ, \mathbf{q}) with $ik_n(iq_\ell) = (2n + 1)\pi/\beta(2\ell\pi/\beta)$ being the Fermi (Bose) Matsubara frequencies, and $\beta = 1/T$ is the inverse temperature. We have introduced Grassmann numbers $\psi_{\alpha\sigma}$ where the flavor label $\alpha = \pm 1$ stands, respectively, for the A and B layers, and $P_\alpha^*(q) = \sum_k \psi_{\alpha\uparrow}^*(q+k) \psi_{\alpha\downarrow}^*(-k)$.

The possibility of a superfluid state is investigated by introducing Hubbard-Stratonovich pair fields $\Delta_\alpha(q)$ to decouple the interaction term (see Appendix A) in Eq. (3). The fermions are then integrated out to obtain the action $S[\Delta]$ solely for $\Delta_\alpha(q)$. The uniform saddle point $\Delta_\alpha^C(q) = \Delta \delta_{q,0}$, where Δ is the superfluid order parameter, gives the gap equation

$$\frac{1}{U} = \frac{1}{N} \sum_k \frac{\tanh \frac{\beta E(k)}{2}}{2E(k)}, \quad (4)$$

where $E(k) = \sqrt{e(\mathbf{k})^2 + \Delta^2}$. The model we consider here has particle-hole symmetry which forces $\mu = 0$ when the occupancy is one fermion per site; thus a separate number equation to determine μ is obviated. Figure 3(a) shows the evolution of the zero-temperature ground state with increasing U . At U_c , a quantum phase transition occurs ushering in a superfluid state where Δ behaves as $\sqrt{U - U_c}$ and monotonically increases with increasing U . The superfluidity arises from the promotion of fermions to the conduction band; indeed, $n = \frac{1}{N} \sum_{k\sigma} \langle c_{k\sigma}^\dagger c_{k\sigma} \rangle$ [see Eq. (1)], the number of fermions promoted to the conduction band increases from zero at U_c as $n \sim (U - U_c)$.

Having established the superfluid ground state and its physical underpinnings, the natural question is regarding the magnitude of the transition temperature of the superfluid

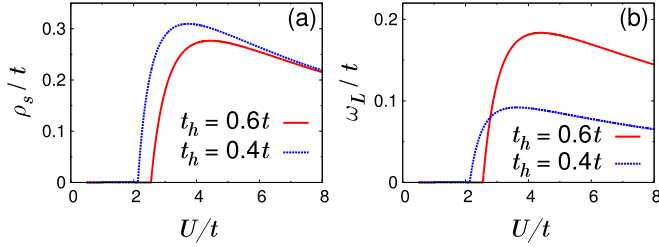


FIG. 4. (Color online) Evolution of (a) superfluid density ρ_s and (b) Leggett mode gap ω_L as a function of U at zero temperature.

obtained. Two effects that destroy superfluidity are pair breaking and phase fluctuations. Indeed, long-wavelength phase fluctuations render our 2D superfluid lacking in true long-range order at finite temperatures, i.e., in the Kosterlitz-Thouless phase. The temperature scale of pair-breaking T_Δ is set by the lowest temperature at which the saddle point value of Δ vanishes and can be obtained by solving for the temperature in the gap equation [Eq. (4)] with $\Delta = 0$. To investigate the role of phase fluctuations below T_Δ and estimate the transition temperature, we study the fluctuations at the Gaussian level (see Appendix A) by expanding the action $\mathcal{S}[\Delta]$ about the saddle point with $\Delta_\alpha(q) = \Delta_\alpha^c(q) + \Delta[\zeta_\alpha(q) + i\theta_\alpha(q)]$, where $\zeta_\alpha(q)$ and $\theta_\alpha(q)$ are real fields that represent, respectively, the amplitude and phase fluctuations in each layer. The fluctuations in each layer are coupled; a more natural “normal mode” description is in terms of symmetric and antisymmetric linear combinations of these modes. For example, there are two phase modes—the symmetric mode $\theta_s(q) \sim [\theta_+(q) + \theta_-(q)]$ and the antisymmetric mode $\theta_a(q) \sim [\theta_+(q) - \theta_-(q)]$, and there are two amplitude modes with similar definition.

We find that both the amplitude modes are gapped, while the symmetric phase mode is gapless and the antisymmetric phase mode is gapped. Interestingly, the gapped antisymmetric phase mode is analogous to the Leggett mode in multiband superconductors [32,33]. We obtain the following effective action for the phase modes by integrating out the amplitude modes $\mathcal{S}[\theta_s, \theta_a] = \int_0^\beta d\tau \int d^2r \frac{1}{2} [(\kappa_s(\frac{\partial \theta_s}{\partial \tau})^2 + \rho_s(\frac{\partial \theta_s}{\partial r})^2) + (\kappa_a(\frac{\partial \theta_a}{\partial \tau})^2 + \rho_a(\frac{\partial \theta_a}{\partial r})^2 + \omega_L \theta_a^2)]$, where τ is the imaginary time, r is the position on the 2D plane, κ 's, ρ 's, and ω_L are determined by the saddle point solution. The most important parameters (Appendix A) in this action are the phase stiffness of the symmetric phase mode ρ_s , which is the superfluid density, and ω_L , the gap (or mass) associated with the antisymmetric Leggett mode. Figure 4(a) shows the dependence of the zero-temperature superfluid density ρ_s on U . For $U \gtrsim U_c$, $\rho_s \sim U - U_c$ and has the same behavior as the number of fermions excited to the conduction band. With increase of U , ρ_s attains a maximum and suffers a fall at larger values of U . For $U \gg t$, we find that $\rho_s \sim \frac{t^2}{U}$. This is due to the fact that the system undergoes a “BCS-BEC” crossover with increasing U , and ρ_s is determined by the hopping amplitude of the bosonic fermion pair at large U , which is $\sim t^2/U$. The variation of ω_L with U is shown in Fig. 4(b), the key point to be noted is that in the regime where ρ_s is the largest, the Leggett mode has a large gap and does not participate in the low-energy physics.

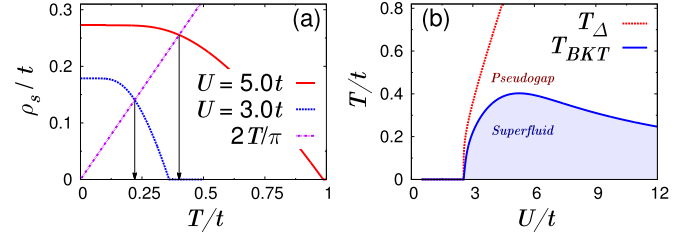


FIG. 5. (Color online) (a) Determination of T_{BKT} from the temperature dependence of ρ_s . (b) Dependence of T_Δ and T_{BKT} on U . Note the high transition temperature and the large pseudogap regime. Here $t_h = 0.9t$.

The discussion above allows the estimation of the Kosterlitz-Thouless transition temperature T_{BKT} . We obtain ρ_s as a function of T via our functional formulation using the saddle-point value of Δ . Using the relationship [34] $\rho_s(T_{\text{BKT}}) = \frac{2T_{\text{BKT}}}{\pi}$, we arrive at the transition temperature [as shown in Fig. 5(a)] plotted in Fig. 5(b), which also shows the temperature T_Δ associated with pair breaking obtained from Eq. (4). We see that the maximum value of T_{BKT} is of the order of the lattice hopping amplitude t (for a potential depth of about $3 - 5E_R$ (recoil energy), highest $T_{\text{BKT}} \approx 0.1E_R$), and in this sense we obtain *high-temperature* superfluidity. Note that the optimum T_{BKT} in our system is about twice larger than that obtained in a single layer [35] attractive Hubbard model [see Appendix B]. The BCS side ($U \gtrsim U_c$) is also a robust superfluid due to the enhancement obtained by the divergent density of states. Another attractive aspect of this system is that one expects to see large pseudogap features even at high temperatures [see Fig. 5(b)], and thus interesting physics can be investigated in optical lattices even if the average entropy of the system is not small.

The effect of quantum fluctuations are likely important due to the reduced dimensionality [36]. To ensure that quantum fluctuations only have a quantitative role and to ensure that there are no competing orders such as a CDW intervening, we conducted a detailed variational Monte Carlo [37–40] calculation of the ground state (see Appendix C). Our variational ground state $|\Psi\rangle = g^D |\Delta_S, \Delta_{\text{CDW}}\rangle_{\text{BCS}}$ is constructed by introducing both the superfluid pair order Δ_S and a commensurate (π, π) charge density wave order parameter Δ_{CDW} , and obtaining the BCS state $|\Delta_S, \Delta_{\text{CDW}}\rangle_{\text{BCS}}$. The Gutzwiller parameter $g (> 1)$ that promotes double occupancy (D is the operator that counts the number of doubly occupied sites) introduces quantum fluctuations of the local phase. Two key results of our detailed study are the following: (i) For all values of U within the range considered here, the optimal value of Δ_{CDW} is zero (also found in a saddle point theory); i.e., there is no competing order that intervenes and hence the superfluid state is stable, and (ii) quantum fluctuations do not change the qualitative aspects of the results. Indeed, for the parameter values shown in Fig. 6(a), we find $U_c \approx 4.5$ is expectedly larger than the value of 3.2 from the saddle point analysis (Appendix C). The variational parameter Δ_S [Fig. 6(a)] and the superfluid order parameter Φ [Fig. 6(b)], which measures the amplitude of injecting a pair at a large distance away from the point of its removal, have precisely the behavior as expected from the saddle point analysis. Superfluidity wins

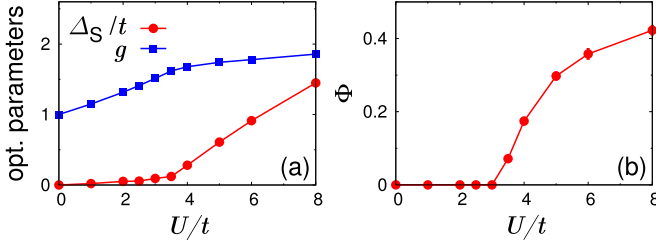


FIG. 6. (Color online) Results of variational Monte Carlo calculations. Dependence of (a) variational parameters g and Δ_S and (b) superfluid order parameter Φ on U . $t_h = 0.9t$.

over other competing orders since the pairing channel has the most divergent susceptibility due to the density of states discussed earlier.

IV. POSSIBLE EXPERIMENTAL REALIZATION AND DISCUSSION

Our proposed scheme can be realized by an “orthogonally shaken bilayer,” depicted in Fig. 7. It is argued in Ref. [41] that upon introducing a shake of the optical lattice, the amplitude and the *sign* of the hopping can be controlled. It was shown that if K (an energy scale) and ν are, respectively, the amplitude and frequency of the shake, the effective hopping amplitude $t_{\text{eff}} = t J_0(\frac{K}{\nu})$, where J_0 is the Bessel function and t is the hopping in the absence of the shake. This phenomenon has not only been observed experimentally [42] but also has been recently used to study many interesting quantum phases [43,44] with further proposals for the generation of topological insulators [45,46].

Our proposed experimental setup consists of two adjacent optical square lattices. The top layer A is obtained by interfering two sets of counter-propagating laser beams in the x and y directions; the x and y beams are noninterfering. The relative phase of the two x laser beams is modulated so as to obtain a shake, and the intensity of the x laser beams and the amplitude of the modulation can be chosen such that $-t_x^A = t_y^A = t$; i.e., the hopping along the x direction has an opposite sign to that in the y direction. In the layer B , the beams along the y direction are shaken so that $t_x^A = -t_y^B = t$. This provides a realization of a system with $\varepsilon_A(\mathbf{k}) = -\varepsilon_B(\mathbf{k})$. The hybridization of the two layers can be controlled by the distance between the two layers. This can be achieved by

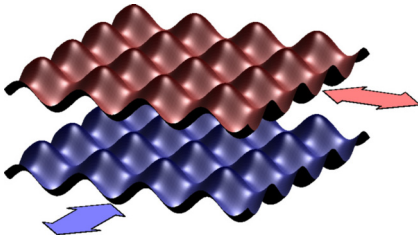


FIG. 7. (Color online) Orthogonally shaken bilayer optical lattice. The top layer A is shaken in the x direction, while the bottom layer B is shaken in the y direction. By an appropriate choice of laser intensities, amplitude, and frequency of the shakes, the band dispersion in the layers can be made to have opposite signs to each other. The layer hybridization can be controlled by the distance between the layers.

using vertically confining beams as in Ref. [47] and creating the two layers by “optical copying.” Optical copying will entail splitting the x and y laser beams of the A layer and focusing the split beams just below the A layer to produce the B layer such that the x beam of the A layer plays the role of the y beam of the B layer, and so on. This laboratory realization of our proposal may require optics techniques that have been used in the making of quantum gas microscopes [48], which will allow for the control of the distance between the two layers. The confining trap potential is to be designed such that a large region near the trap center will be in a band-insulating state, with the excess entropy trapped in regions at the periphery (see Appendix D). Tuning of the attractive interactions [49] should now drive the central band-insulating region to the superfluid state. We hope that this work stimulates experimental research on realizing such a bilayer band insulator system, even by routes other than our proposal.

ACKNOWLEDGMENTS

Y.P. and A.M. thank CSIR and IISc-CPDF, respectively, for support. V.B.S. is grateful to DST (Ramanujan Grant) and DAE-SRC for generous support. The authors thank Tilman Esslinger for discussions and suggestions regarding experimental realization of the proposed model, Jayantha Vyasanakere for discussions and comments, and Arun Paramakanti for comments on the manuscript.

APPENDIX A: GAUSSIAN THEORY OF THE SUPERFLUID STATE

The Hamiltonian of our proposed *bilayer band insulator model* consists of two parts $\mathcal{H} = \mathcal{H}_K + \mathcal{H}_U$, where \mathcal{H}_K and \mathcal{H}_U are defined in the main text.

In the functional integral framework, we write the action

$$\mathcal{S}[\psi] = \sum_{k,k',\alpha} \psi_{\alpha\sigma}^*(k) [-G_{0,\alpha\sigma,\alpha'\sigma'}^{-1}(k,k')] \psi_{\alpha'\sigma'}(k') - \frac{U}{\beta N} \sum_{q,\alpha} P_{\alpha}^*(q) P_{\alpha}(q), \quad (\text{A1})$$

where

$$G_0^{-1}(k,k') = \{ik_n \mathbb{1} \otimes \mathbb{I} - [\alpha\varepsilon(\mathbf{k})\tau_z \otimes \sigma_z - t_h \tau_x \otimes \sigma_z]\} \Delta_{kk'}. \quad (\text{A2})$$

Here $\mathbb{1}$ and τ 's are, respectively, the identity and Pauli matrices in $1 - \bar{1}$ ($A-B$ or $+$ and $-$) space. Similarly \mathbb{I} and σ 's are the identity and Pauli matrices in spin space. We note that the $1 - \bar{1}$ and $+$ and $-$ notations for the layer index are used interchangeably depending on typographical convenience.

We now decouple the four-fermion interaction term by introducing a Hubbard-Stratonovich pair field, $\Delta_{\alpha}(q)$. This decoupling results in the action

$$\mathcal{S}[\psi, \Delta] = \sum_{k,k',\alpha} \psi_{\alpha\sigma}^*(k) [-G_{\alpha\sigma,\alpha'\sigma'}^{-1}(k,k')] \psi_{\alpha'\sigma'}(k') + \frac{1}{U} \sum_{q,\alpha} \Delta_{\alpha}^*(q) \Delta_{\alpha}(q), \quad (\text{A3})$$

where $G_{\alpha\sigma,\alpha'\sigma'}^{-1}(k,k') = G_{0\alpha\sigma,\alpha'\sigma'}^{-1}(k,k') - \Delta(k,k')$,

$$\Delta(k,k') = \begin{bmatrix} 0 & 0 & \Delta_+(k,k') & 0 \\ 0 & 0 & 0 & \Delta_-(k,k') \\ \Delta_+^*(k,k') & 0 & 0 & 0 \\ 0 & \Delta_-^*(k,k') & 0 & 0 \end{bmatrix}, \quad (\text{A4})$$

with $\Delta_\alpha(k,k') = \frac{1}{\sqrt{\beta N}} \sum_q \Delta_\alpha(q) \Delta_{q,k-k'}$. The fermions are integrated out to obtain the action only in terms of the pairing field,

$$S[\Delta] = \frac{1}{U} \sum_{q,\alpha} \Delta_\alpha^*(q) \Delta_\alpha(q) - \ln \det[-G^{-1}(\Delta)]. \quad (\text{A5})$$

We perform a saddle-point analysis with an ansatz $\Delta_\alpha^C(q) = \Delta_{q,0}$, where Δ is chosen to be real without loss of generality. Within this ansatz, the Green's function $G(k,k')$ has the form

$$G(k,k') = \frac{\Delta_{kk'}}{(ik_n)^2 - E(\mathbf{k})^2} \{ ik_n \mathbb{1} \otimes \mathbb{I} + [\varepsilon(\mathbf{k})\tau_z \otimes \sigma_z - t_h \tau_x \otimes \sigma_z] + \Delta \mathbb{1} \otimes \sigma_z \}, \quad (\text{A6})$$

where $E(\mathbf{k})$ is defined near the gap equation [Eq. (4)]. The gap equation is obtained by extremizing the action with respect to Δ ; Equation (4) is obtained after the necessary frequency sums.

The important role of fluctuations is explored by a Gaussian theory. We expand the action $S[\Delta]$ about the saddle point with $\Delta_\alpha(q) = \Delta^C(q)_\alpha + \eta_\alpha(q)$ and retain terms up to quadratic order in the fluctuation η_α in the action (repeated α and β indices are summed)

$$S[\eta] = S^{\text{sp}} + \frac{1}{2} \sum_q [\eta_\alpha^*(q) \eta_\alpha(-q)] \mathbf{\Pi}(q) \begin{bmatrix} \eta_\beta(q) \\ \eta_\beta^*(-q) \end{bmatrix}, \quad (\text{A7})$$

where

$$\mathbf{\Pi}(q) = \begin{bmatrix} C_{\alpha\beta}(q) & D_{\alpha\beta}(q) \\ A_{\alpha\beta}(-q) & B_{\alpha\beta}(-q) \end{bmatrix}, \quad (\text{A8})$$

with

$$C_{\alpha\beta}(q) = \frac{1}{\beta N} \sum_k G_{\alpha\uparrow,\beta\uparrow}(k+q) G_{\alpha\downarrow,\beta\downarrow}(k) + \frac{\Delta_{\alpha,\beta}}{U} \\ = B_{\beta\alpha}(q) \quad (\text{A9})$$

and

$$D_{\alpha\beta}(q) = \frac{1}{\beta N} \sum_k G_{\alpha\uparrow,\beta\downarrow}(k+q) G_{\alpha\downarrow,\beta\uparrow}(k) = A_{\alpha\beta}(q). \quad (\text{A10})$$

We now express the η fields in terms of two other real fields ζ (amplitude fluctuation) and θ (phase fluctuation) as $\eta_\alpha(q) = \Delta[\zeta_\alpha(q) + i\theta_\alpha(q)]$, with $\zeta^*(q) = \zeta(-q)$ and $\theta^*(q) = \theta(-q)$, to study both amplitude and phase fluctuations. The action in terms of these two fields is

$$S[\zeta,\theta] = S^{\text{sp}} + \frac{1}{2} \sum_q [\zeta_\alpha^*(q) \theta_a^*(q)] \mathbf{\Gamma}(q) \begin{bmatrix} \zeta_\beta(q) \\ \theta_\beta(q) \end{bmatrix}, \quad (\text{A11})$$

where

$$\mathbf{\Gamma}(q) = \begin{bmatrix} \Gamma_{\zeta\zeta}^{\alpha\beta}(q) & \Gamma_{\zeta\theta}^{\alpha\beta}(q) \\ \Gamma_{\theta\zeta}^{\alpha\beta}(q) & \Gamma_{\theta\theta}^{\alpha\beta}(q) \end{bmatrix}, \quad (\text{A12})$$

$$\Gamma_{\zeta\zeta}^{\alpha\beta}(q) = \Delta^2 [C_{\alpha\beta}(q) + C_{\alpha\beta}(-q) + D_{\alpha\beta}(q) + D_{\alpha\beta}(-q)], \quad (\text{A13})$$

$$\Gamma_{\zeta\theta}^{\alpha\beta}(q) = i\Delta^2 [C_{\alpha\beta}(q) - C_{\alpha\beta}(-q)] = -\Gamma_{\theta\zeta}^{\alpha\beta}(q), \quad (\text{A14})$$

$$\Gamma_{\theta\theta}^{\alpha\beta}(q) = \Delta^2 \{ [C_{\alpha\beta}(q) + C_{\alpha\beta}(-q)] - [D_{\alpha\beta}(q) + D_{\alpha\beta}(-q)] \}. \quad (\text{A15})$$

As is evident, the phase and amplitude modes of each of the + and - layers are coupled with each other. It is more natural to describe the amplitude and phase modes of each the + and - layers in terms of “normal modes”—these are the symmetric and antisymmetric modes of the phase and amplitude modes of the two layers. Thus, the two phase degrees of freedom are the symmetric mode $\theta_s(q) = [\theta_+(q) + \theta_-(q)]/2$ and the antisymmetric mode $\theta_a(q) = [\theta_+(q) - \theta_-(q)]/2$. Similarly, two amplitude modes can be expressed as the symmetric mode $\zeta_s(q) = [\zeta_+(q) + \zeta_-(q)]/2$ and the antisymmetric mode $\zeta_a(q) = [\zeta_+(q) - \zeta_-(q)]/2$. The action in terms of these symmetric and antisymmetric ζ and θ fields is

$$S[\zeta_s, \zeta_a, \theta_s, \theta_a] = \frac{1}{2} \sum_q [\zeta_s^*(q) \zeta_a^*(q) \theta_s^*(q) \theta_a^*(q)] \mathbf{\Lambda}(q) \begin{bmatrix} \zeta_s(q) \\ \zeta_a(q) \\ \theta_s(q) \\ \theta_a(q) \end{bmatrix}, \quad (\text{A16})$$

where

$$\mathbf{\Lambda}(q) = \begin{bmatrix} L_s(q) & 0 & H_s(q) & 0 \\ 0 & L_a(q) & 0 & H_a(q) \\ K_s(q) & 0 & H_s(q) & 0 \\ 0 & K_a(q) & 0 & H_a(q) \end{bmatrix}, \quad (\text{A17})$$

with $L_{s,a}$ and $H_{s,a}$ being appropriate linear combinations of Γ 's defined above. Thus the action splits nicely into the symmetric and antisymmetric modes, $S[\zeta_s, \zeta_a, \theta_s, \theta_a] = S_a[\zeta_s, \theta_s] + S_s[\zeta_a, \theta_a]$; i.e., the symmetric and antisymmetric modes do not interact with each other. After performing the necessary frequency sums to obtain the expressions for the L 's, H 's, and K 's, we find that both symmetric and antisymmetric amplitude modes are gapped. Also, the antisymmetric phase mode is gapped and the symmetric phase mode is gapless. Since the amplitude modes are gapped, we integrate them out to obtain a “phase-only” action. This action (apart from constants) is

$$S_{\text{eff}}[\theta_s, \theta_a] = S^{\text{sp}} + \frac{1}{2} \sum_q \theta_s^* \tilde{K}_s(q) \theta_s + \theta_a^* \tilde{K}_a(q) \theta_a, \quad (\text{A18})$$

where $\tilde{K}_s = K_s - \frac{H_s^2}{L_s}$ and $\tilde{K}_a = K_a - \frac{H_a^2}{L_a}$. For small q , we find $\tilde{K}_s = \rho_s q^2 - (iq_l)^2 \kappa$ and $\tilde{K}_a = \tilde{K}_s + \omega_L$, where ρ_s is the

superfluid density, given by

$$\rho_s = \frac{2\Delta^2}{N} \sum_{\mathbf{k}} \frac{v_x(\mathbf{k})v_x(\mathbf{k})}{4E(\mathbf{k})^2} \times \left[2 \frac{\partial n_F(E(\mathbf{k}))}{\partial E(\mathbf{k})} + \frac{1 - 2n_F(E(\mathbf{k}))}{E(\mathbf{k})} \right], \quad (\text{A19})$$

where $v_x(\mathbf{k}) = \alpha \partial e(\mathbf{k}) / \partial k_x$ is the velocity and ω_L is the gap of the asymmetric phase (Leggett) mode, given by

$$\omega_L = \frac{8t_h^2 \Delta^2}{N} \sum_{\mathbf{k}} \frac{1}{4E(\mathbf{k})^2} \left[2 \frac{\partial n_F(E(\mathbf{k}))}{\partial E(\mathbf{k})} + \frac{1 - 2n_F(E(\mathbf{k}))}{E(\mathbf{k})} \right], \quad (\text{A20})$$

with n_F being the Fermi function. We do not show expressions for κ and other quantities, all of which depend on the saddle-point value Δ in analogous fashion as above. Equation (A18) transformed to space and imaginary time is shown in the text, with $\rho_a = \rho_s$ and $\kappa_a = \kappa_s = \kappa$.

APPENDIX B: COMPARIAON OF BILAYER SYSTEM WITH SINGLE-LAYER ATTRACTIVE HUBBARD MODEL

In this section, we present a comparison of the physics of the bilayer system with a single-layer attractive Hubbard model (AHM).

The key point to be noted is that our bilayer band insulator system produces a system with a higher superfluid density. This enhancement arises from the fact that the orthogonal phase modes of our system are the symmetric and antisymmetric modes. The antisymmetric mode, the Leggett mode, is *gapped* and hence the low-energy physics is governed solely by the symmetric mode. The symmetric mode corresponds to the simultaneous twisting of the phase in *two layers*, each with a filling of one particle per site. This then makes our $\rho_s \approx 2\rho_s^{\text{AHM}}$ and engenders an enhanced T_c . Note also, that this is also consistent with the following well-known sum rule which states that, in a lattice, $\rho_s \sim \langle \text{kinetic energy} \rangle$. Our system with two layers has roughly twice the kinetic energy as a single-layer AHM.

In Fig. 8, we compare the T_c of our system with AHM cacluated with *same* formulation. We see the *expected* enhancement of the T_{BKT} of our bilayer system, over the

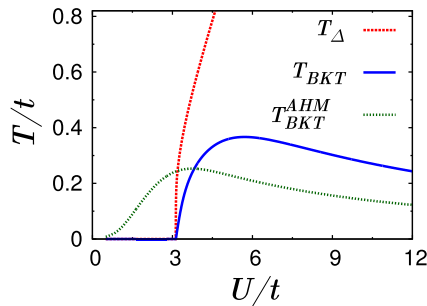


FIG. 8. (Color online) T_Δ and T_{BKT} are for the bilayer system with $t_h = 0.9t$. $T_{\text{BKT}}^{\text{AHM}}$ is for the single-layer AHM at half filling. Note that the highest T_{BKT} of the bilayer system is about a factor of 2 larger than that obtained in the single-layer AHM.

AHM. We note here that the T_{BKT} of the AHM model matches published values [35].

The advantage of the bilayer system over the AHM for the realization of an optical lattice superfluid is now evident. In the AHM, the one-particle excitations are gapless in the absence of U . Thus even in the starting state, the high initial entropy of the system will be spread throughout the trap. In contrast, in our proposal the central region of the trap will continue to be a low-entropy state, and the added bonus of a high-transition-temperature realization of the superfluid-pseudogap state is made more favorable.

APPENDIX C: VARIATIONAL MONTE CARLO CALCULATIONS OF THE GROUND STATE

To study the effects of quantum fluctuations, we do a variational Monte Carlo (VMC) calculation by taking the following as our variational wave function for the ground state:

$$|\Psi_{\text{var}}\rangle = g^D \mathcal{P}_N |\Delta_S, \Delta_{\text{CDW}}\rangle_{\text{BCS}}. \quad (\text{C1})$$

Here g is the Gutzwiller factor,

$$D = \sum_i (a_{i\uparrow}^\dagger a_{i\downarrow}^\dagger a_{i\downarrow} a_{i\uparrow} + b_{i\uparrow}^\dagger b_{i\downarrow}^\dagger b_{i\downarrow} b_{i\uparrow}) \quad (\text{C2})$$

is the number of doubly occupied sites, and \mathcal{P}_N is the fixed electron number (N) projection operator. The wave function $|\Delta_S, \Delta_{\text{CDW}}\rangle_{\text{BCS}}$ is the ground state of the following Hamiltonian which incorporates the pairing and CDW orders simultaneously,

$$\begin{aligned} \mathcal{H}_{\text{MF}} = & \sum_{k\sigma} \varepsilon_k (a_{k\sigma}^\dagger a_{k\sigma} - b_{k\sigma}^\dagger b_{k\sigma}) - t_h \sum_{k\sigma} (a_{k\sigma}^\dagger b_{k\sigma} + \text{H.c.}) \\ & - \Delta_S \sum_i (a_{i\uparrow}^\dagger a_{i\downarrow}^\dagger + b_{i\uparrow}^\dagger b_{i\downarrow}^\dagger + \text{H.c.}) \\ & - \Delta_{\text{CDW}} \sum_{i\sigma} \cos(\mathbf{Q} \cdot \mathbf{r}_i) (a_{i\sigma}^\dagger a_{i\sigma} - b_{i\sigma}^\dagger b_{i\sigma}). \end{aligned} \quad (\text{C3})$$

Here $\mathbf{Q} = (\pi, \pi)$ and the chemical potential $\mu = 0$ as demanded by particle-hole symmetry. The above Hamiltonian can be diagonalized via a Bogoliubov transformation and the final form of the ground-state wave function is

$$|\Delta_S, \Delta_{\text{CDW}}\rangle_{\text{BCS}} = \prod_k \prod_{n=1}^4 (u_{kn} + v_{kn} f_{kn\uparrow}^\dagger f_{-kn\downarrow}^\dagger) |0\rangle, \quad (\text{C4})$$

where u_{kn} and v_{kn} are dependent on the parameters Δ_S and Δ_{CDW} , and $f_{kn\sigma}$'s are the operators obtained after transforming the original electron operators. Upon application of the projection operator \mathcal{P}_N , the wave function is

$$|\Psi_{\text{var}}(g, \Delta_S, \Delta_{\text{CDW}})\rangle = g^D \left(\sum_{kn} \phi_{kn} f_{kn\uparrow}^\dagger f_{-kn\downarrow}^\dagger \right)^{N/2} |0\rangle, \quad (\text{C5})$$

which contains three parameters, e.g., g , Δ_S , and Δ_{CDW} . In order to determine the ground state, we calculate the variational energy,

$$E(g, \Delta_S, \Delta_{\text{CDW}}) = \frac{\langle \Psi_{\text{var}} | \mathcal{H} | \Psi_{\text{var}} \rangle}{\langle \Psi_{\text{var}} | \Psi_{\text{var}} \rangle}, \quad (\text{C6})$$

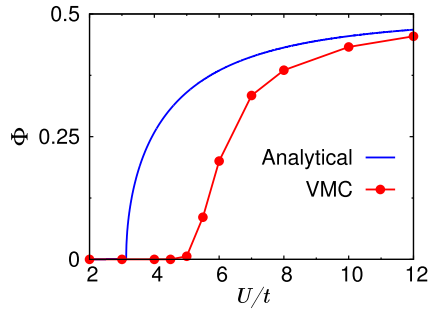


FIG. 9. (Color online) Comparison of analytical theory with the VMC calculation of the order parameter. U_c in the VMC is larger than that obtained in U_c with $t_h = 0.9t$.

using VMC and optimize it in the space of the above three parameters. We do the calculations on a lattice of size $10 \times 10 \times 2$.

After careful optimization of the variational energy, we find that up to $U = 8t$, the minimum energy is obtained when $\Delta_{\text{CDW}} = 0$. Thus within this range of U , the CDW state is ruled out as a competing order in the ground state in agreement with the conclusion from the mean-field calculation. The optimal values of g and Δ_S as a function of U are shown in Fig. 6(a). Once the wave function is optimized, we estimate the pairing order parameter of the system by calculating the pair correlation function $F(\mathbf{r} - \mathbf{r}')$, given by

$$F(\mathbf{r} - \mathbf{r}') = \langle c_{r\uparrow}^\dagger c_{r\downarrow}^\dagger c_{r'\uparrow} c_{r'\downarrow} \rangle. \quad (\text{C7})$$

Here the operators $c_{r\sigma}$ mean either $a_{r\sigma}$ or $b_{r\sigma}$. The pairing order parameter Φ is obtained from long-range behavior of the pair correlation function as

$$\Phi^2 = \lim_{|\mathbf{r}-\mathbf{r}'| \rightarrow \infty} F(\mathbf{r} - \mathbf{r}'). \quad (\text{C8})$$

The pairing order parameter thus obtained is shown in Fig. 6(b) as a function of U . It is interesting to note that though the optimal Δ_S is nonzero as soon as $U > 0$, the superconducting order develops only after a critical value U_c .

Figure 9 shows a comparison of the order parameter Φ as a function of U/t for the VMC and analytical theory. As expected, we find that $U_c/t|_{\text{VMC}} (= 4.5) > U_c/t|_{\text{MFT}} (3.2)$, and the qualitative aspect Φ has excellent agreement between the two. This discussion produces the expected conclusion that quantum fluctuations influence only the quantitative aspects, i.e., a larger U_c , while the qualitative aspects are identical to those obtained by the analytical theory.

APPENDIX D: DISCUSSION OF EXPERIMENTAL REALIZATION

Our proposal for the realization of the fermionic superfluid state relies on two aspects, namely, that the characteristic temperature of the many-body state realized in the system is large and also that the low-entropy state provides a method to spatially accommodate the initial entropy in the periphery of the trap. In the presence of the trapping potential, the state realized in our system will correspond to the half-filled bilayer in the central (inner) region of the trap, while the outer region will be of lower density. Thus the outer “metallic” regions with gapless one-particle excitations will have a higher entropy density (due to its large specific heat), while the inner core will be the band insulator with a low-entropy density. Ramping an attractive interaction will drive the band-insulating region to a superfluid state. The outer region will be in a normal state with pairing fluctuations brought about by the attractive interaction. This would then be analogous to the realization of a superfluid in the continuum system in a trap where the inside core is superfluid and the outside is normal [1].

-
- [1] W. Ketterle and M. W. Zwierlein, in *Proceedings of the International School of Physics “Enrico Fermi,” Course CLXIV, Varenna, 2006*, edited by M. Inguscio, W. Ketterle, and C. Salomon (IOS Press, Amsterdam, 2008).
- [2] I. Bloch, J. Dalibard, and W. Zwerger, *Rev. Mod. Phys.* **80**, 885 (2008).
- [3] S. Giorgini, L. P. Pitaevskii, and S. Stringari, *Rev. Mod. Phys.* **80**, 1215 (2008).
- [4] T. Esslinger, *Annu. Rev. Condens. Matter Phys.* **1**, 129 (2010).
- [5] I. Bloch, J. Dalibard, and S. Nascimbene, *Nat. Phys.* **8**, 267 (2012).
- [6] Y.-J. Lin, R. L. Compton, A. R. Perry, W. D. Phillips, J. V. Porto, and I. B. Spielman, *Phys. Rev. Lett.* **102**, 130401 (2009).
- [7] Y.-J. Lin, R. L. Compton, K. Jimenez-Garcia, J. V. Porto, and I. B. Spielman, *Nature (London)* **462**, 628 (2009).
- [8] Y.-J. Lin, K. Jimenez-Garcia, and I. B. Spielman, *Nature (London)* **471**, 83 (2011).
- [9] P. Wang, Z.-Q. Yu, Z. Fu, J. Miao, L. Huang, S. Chai, H. Zhai, and J. Zhang, *Phys. Rev. Lett.* **109**, 095301 (2012).
- [10] L. W. Cheuk, A. T. Sommer, Z. Hadzibabic, T. Yefsah, W. S. Bakr, and M. W. Zwierlein, *Phys. Rev. Lett.* **109**, 095302 (2012).
- [11] D. C. McKay and B. DeMarco, *Rep. Prog. Phys.* **74**, 054401 (2011).
- [12] B. Capogrosso-Sansone, S. G. Söyler, N. Prokof'ev, and B. Svistunov, *Phys. Rev. A* **77**, 015602 (2008).
- [13] T.-L. Ho and Q. Zhou, *Proc. Natl. Acad. Sci. USA* **106**, 6916 (2009).
- [14] T.-L. Ho and Q. Zhou, [arXiv:0911.5506](https://arxiv.org/abs/0911.5506).
- [15] J.-S. Bernier, C. Kollath, A. Georges, L. De Leo, F. Gerbier, C. Salomon, and M. Köhl, *Phys. Rev. A* **79**, 061601 (2009).
- [16] A. Rosch, D. Rasch, B. Binz, and M. Vojta, *Phys. Rev. Lett.* **101**, 265301 (2008).
- [17] T. Paiva, Y. L. Loh, M. Randeria, R. T. Scalettar, and N. Trivedi, *Phys. Rev. Lett.* **107**, 086401 (2011).
- [18] C. J. M. Mathy, D. A. Huse, and R. G. Hulet, *Phys. Rev. A* **86**, 023606 (2012).
- [19] J. K. Chin, D. E. Miller, Y. Liu, C. Stan, W. Setiawan, C. Sanner, K. Xu, and W. Ketterle, *Nature (London)* **443**, 961 (2006).
- [20] M. Kohmoto and Y. Takada, *J. Phys. Soc. Jpn.* **59**, 1541 (1990).
- [21] P. Nozières and F. Pistolesi, *Eur. Phys. J. B* **10**, 649 (1999).
- [22] H. Zhai and T.-L. Ho, *Phys. Rev. Lett.* **99**, 100402 (2007).
- [23] E. G. Moon, P. Nikolic, and S. Sachdev, *Phys. Rev. Lett.* **99**, 230403 (2007).

- [24] A. A. Burkov and A. Paramekanti, *Phys. Rev. A* **79**, 043626 (2009).
- [25] P. Nikolic, A. A. Burkov, and A. Paramekanti, *Phys. Rev. B* **81**, 012504 (2010).
- [26] P. Nikolic, *Phys. Rev. B* **83**, 064523 (2011).
- [27] C. Chin, R. Grimm, P. Julienne, and E. Tiesinga, *Rev. Mod. Phys.* **82**, 1225 (2010).
- [28] L. N. Cooper, *Phys. Rev.* **104**, 1189 (1956).
- [29] J. P. Vyasanakere and V. B. Shenoy, *Phys. Rev. B* **83**, 094515 (2011).
- [30] C. A. R. Sá de Melo, M. Randeria, and J. R. Engelbrecht, *Phys. Rev. Lett.* **71**, 3202 (1993).
- [31] N. Dupuis, *Phys. Rev. B* **70**, 134502 (2004).
- [32] A. J. Leggett, *Prog. Theor. Phys.* **36**, 901 (1966).
- [33] E. Zhao and A. Paramekanti, *Phys. Rev. Lett.* **97**, 230404 (2006).
- [34] P. M. Chaikin and T. C. Lubensky, *Principles of Condensed Matter Physics* (Cambridge University Press, Cambridge, UK, 1995).
- [35] P. J. H. Denteneer, G. An, and J. M. J. van Leeuwen, *Europhys. Lett.* **16**, 5 (1991).
- [36] A. Paramekanti, M. Randeria, T. V. Ramakrishnan, and S. S. Mandal, *Phys. Rev. B* **62**, 6786 (2000).
- [37] H. Yokoyama and H. Shiba, *J. Phys. Soc. Jpn.* **56**, 1490 (1987).
- [38] S. Pathak, V. B. Shenoy, M. Randeria, and N. Trivedi, *Phys. Rev. Lett.* **102**, 027002 (2009).
- [39] S. Pathak, V. B. Shenoy, and G. Baskaran, *Phys. Rev. B* **81**, 085431 (2010).
- [40] Y. Fujihara, A. Koga, and N. Kawakami, *Phys. Rev. A* **81**, 063627 (2010).
- [41] A. Eckardt, C. Weiss, and M. Holthaus, *Phys. Rev. Lett.* **95**, 260404 (2005).
- [42] H. Lignier, C. Sias, D. Ciampini, Y. Singh, A. Zenesini, O. Morsch, and E. Arimondo, *Phys. Rev. Lett.* **99**, 220403 (2007).
- [43] A. Eckardt, P. Hauke, P. Soltan-Panahi, C. Becker, K. Sengstock, and M. Lewenstein, *Europhys. Lett.* **89**, 10010 (2010).
- [44] J. Struck, C. Ölschläger, R. Le Targat, P. Soltan-Panahi, A. Eckardt, M. Lewenstein, P. Windpassinger, and K. Sengstock, *Science* **333**, 996 (2011).
- [45] P. Hauke, O. Tieleman, A. Celi, C. Ölschläger, J. Simonet, J. Struck, M. Weinberg, P. Windpassinger, K. Sengstock, M. Lewenstein, and A. Eckardt, *Phys. Rev. Lett.* **109**, 145301 (2012).
- [46] J. Struck, C. Ölschläger, M. Weinberg, P. Hauke, J. Simonet, A. Eckardt, M. Lewenstein, K. Sengstock, and P. Windpassinger, *Phys. Rev. Lett.* **108**, 225304 (2012).
- [47] N. Gemelke, X. Zhang, C.-L. Hung, and C. Chin, *Nature (London)* **460**, 995 (2009).
- [48] W. S. Bakr, A. Peng, M. E. Tai, R. Ma, J. Simon, J. I. Gillen, S. Fölling, L. Pollet, and M. Greiner, *Science* **329**, 547 (2010).
- [49] For adiabaticity, the ramp time τ_R of U from zero to U_c for typical parameter values should satisfy $\tau_R \gtrsim \frac{\ln 2}{\Gamma}$. This should be readily achievable in experiment.